Hdac4 interactions in Huntington's Disease viewed through the prism of multiomics

Joel D. Federspiel, Todd M. Greco, Krystal K. Lum, and Ileana M. Cristea*

* Corresponding author:
Ileana M. Cristea
210 Lewis Thomas Laboratory
Department of Molecular Biology
Princeton University
Princeton, NJ 08544
Tel: 6092589417
Fax: 6092584575

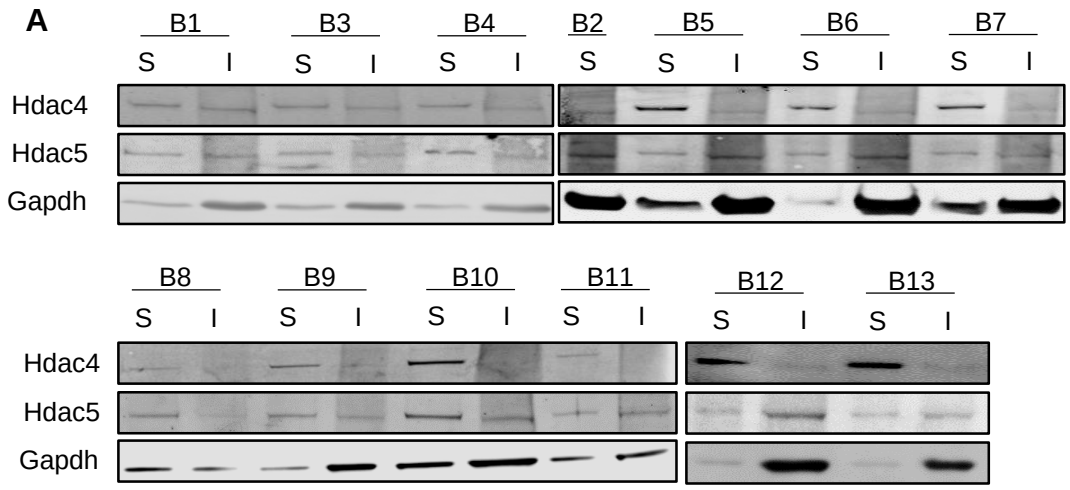

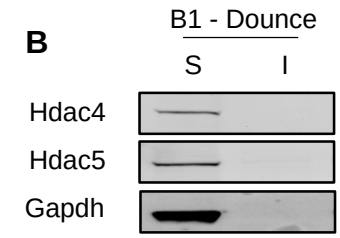

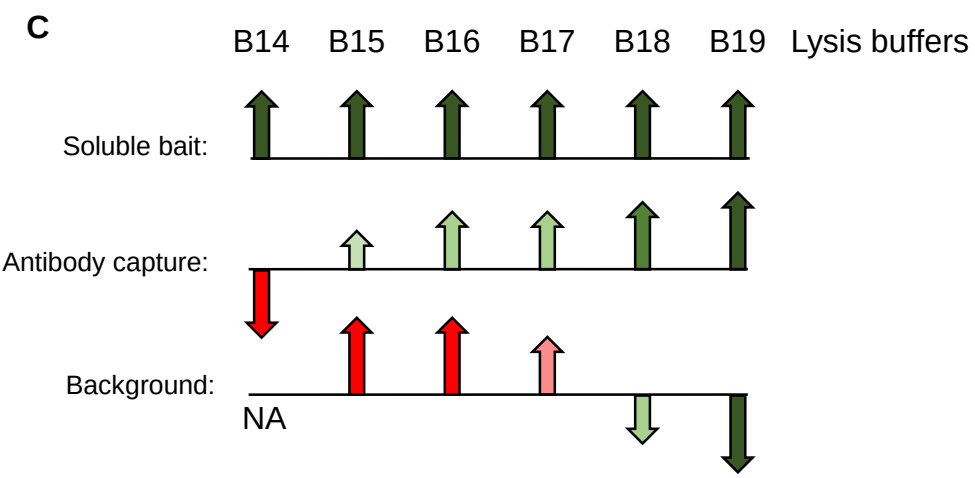

Figure S1. **Optimization of lysis and IP conditions**. (A) Western blots of Hdac4 and Hdac4 soluble (S) and insoluble (I) fractions following solubilization from cryoground tissue in different lysis buffers. (B) Efficiency Hdac solubilization of dounce based lysis. (C) Effect of different lysis buffer compositions on antibody capture and background binding. B19 exhibited the most efficient antibody capture with the lowest overall background.

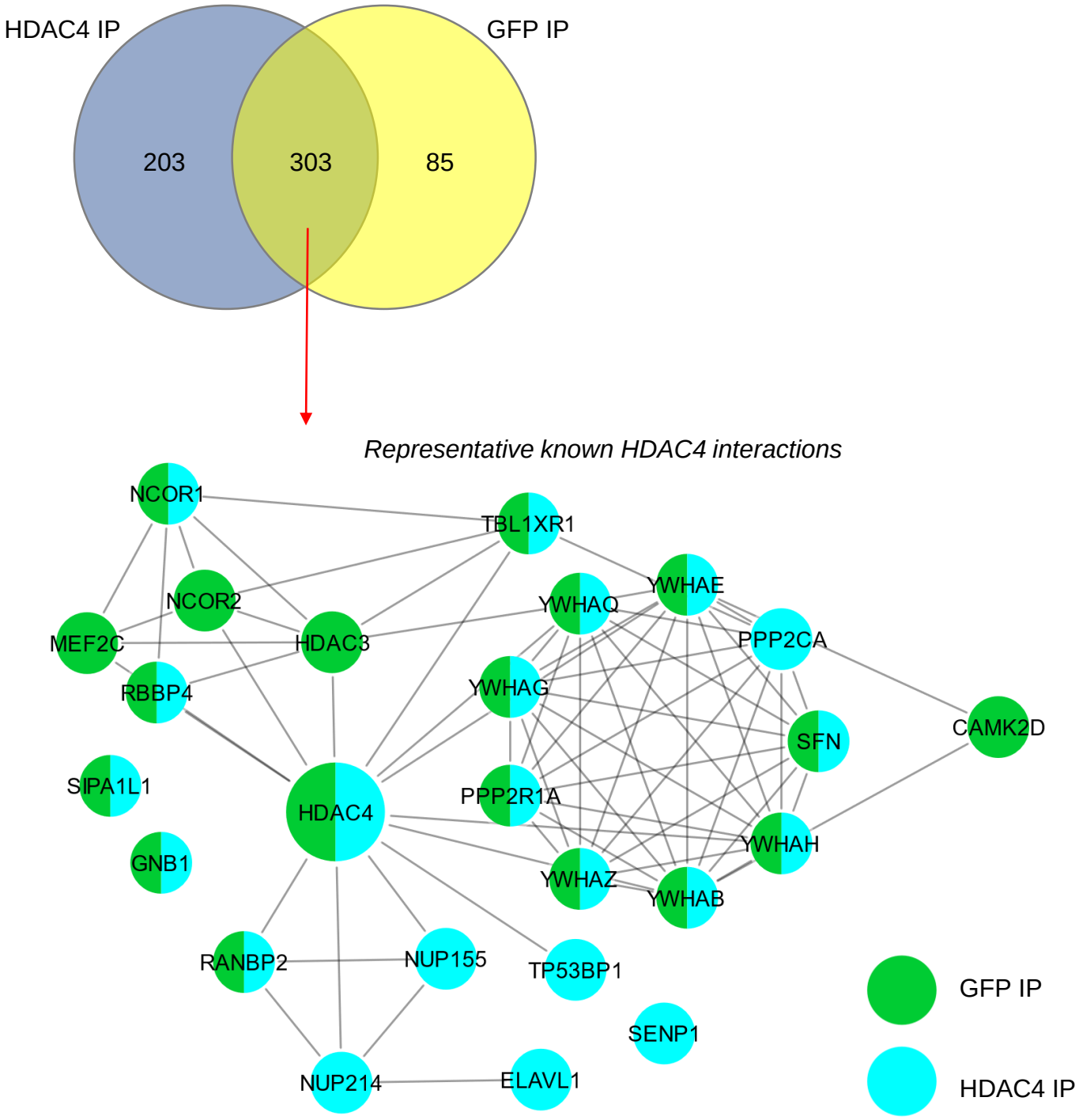

Figure S2. **HDAC4 interactions in CEM-T cells.** The same lysis and IP conditions used in whole brain IPs was used in HDAC4-GFP expressing CEM-T cells with both a GFP IP and an IP using anti-HDAC4. The Venn diagrams illustrate the overall numbers of identified proteins, without specificity filtering. The proteins detected as common between the two IPs included known nuclear HDAC4 interactions. The differences in the proteins co-isolated by either the anti-endogenous HDAC4 or anti-GFP antibody can derive from the binding of the antibodies to different epitopes, as well as different antibody affinities and cross-reactivity. The interaction network shows well-established HDAC4 interactions from previous studies in cells with known nuclear localization for HDAC4.

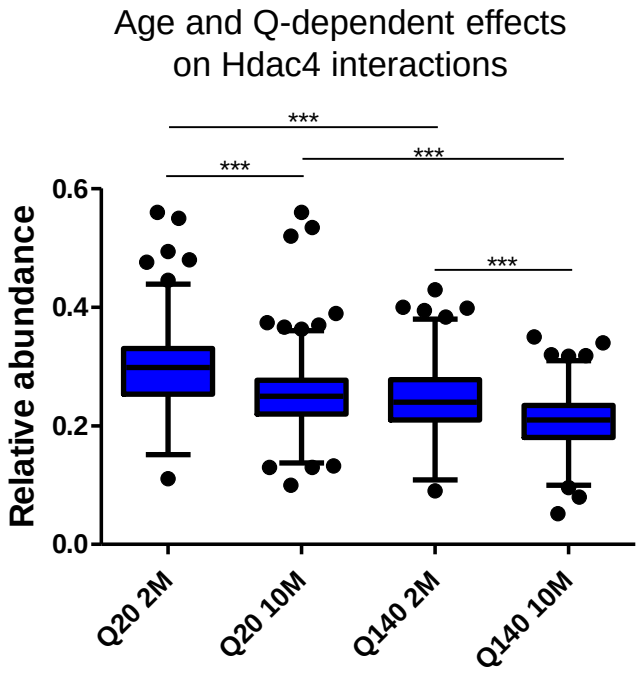

Figure S3. Age and Q-dependent effects on Hdac4 interactions at an alternate threshold. When a uniform SAINT score threshold of ≥0.8 is used across all Hdac4 IPs in whole brain, similar overall trends to Fig 3A are observed.

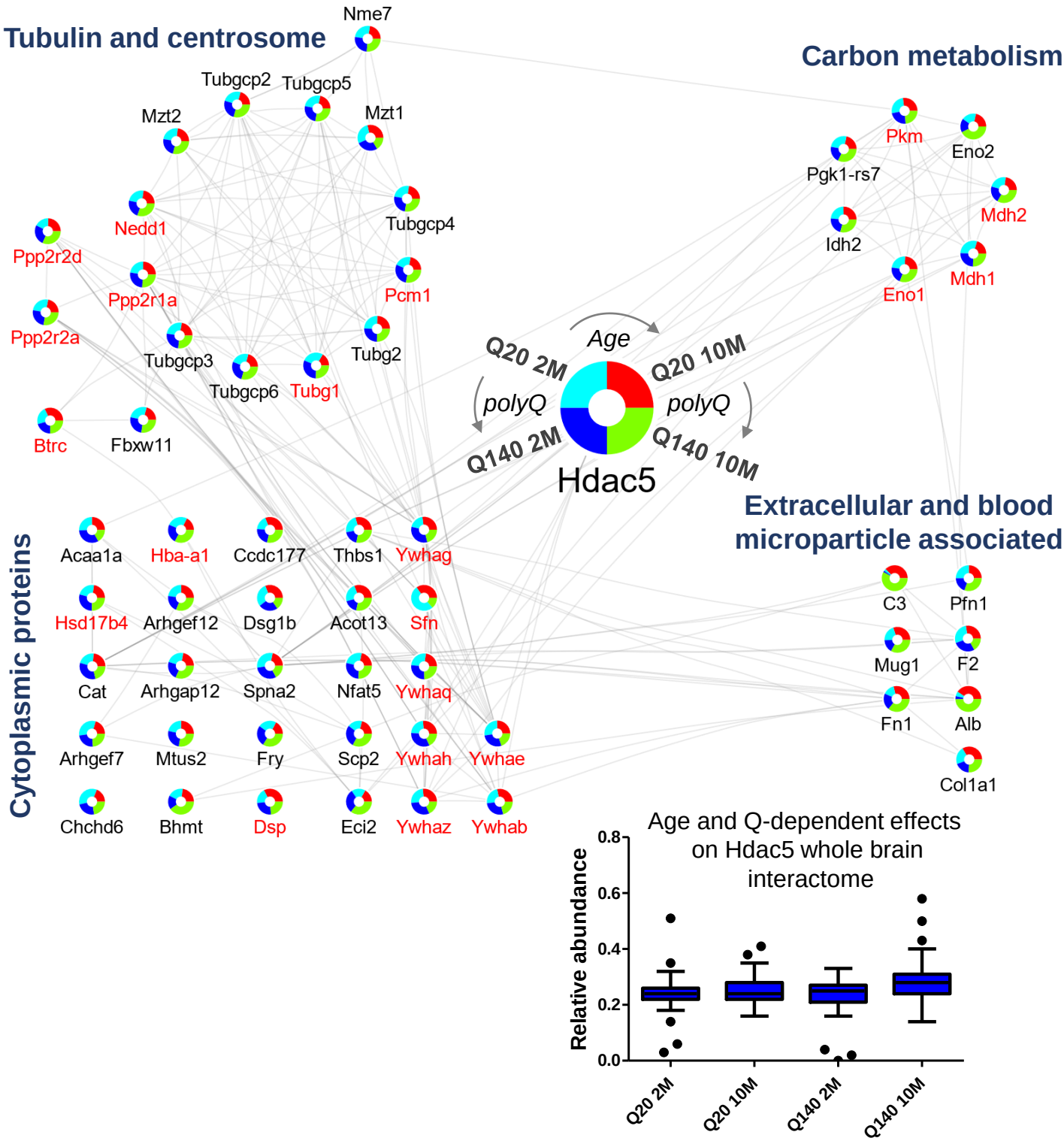

Figure S4. Hdac5 specificity filtered network in whole brain. Comparison of endogenous Hdac5 interactions in Q20 and Q140 mice at 2 and 10 months of age. Each interacting protein is shown as a ring plot with the relative median MS1 abundance levels in each isolation condition depicted as indicated on the Hdac5 ring at the center of the network. Gene names shown in red are Hdac5 specific interactions that are also reported Htt interactions. Edges represent known protein-protein interactions and other associations present in the STRING database. Protein interactions have been functionally grouped and labelled in blue text. Inset boxplot shows overall Hdac5 interaction distribution in whole brain IPs.

IP efficiency blots for all ages and Q lengths – Striata

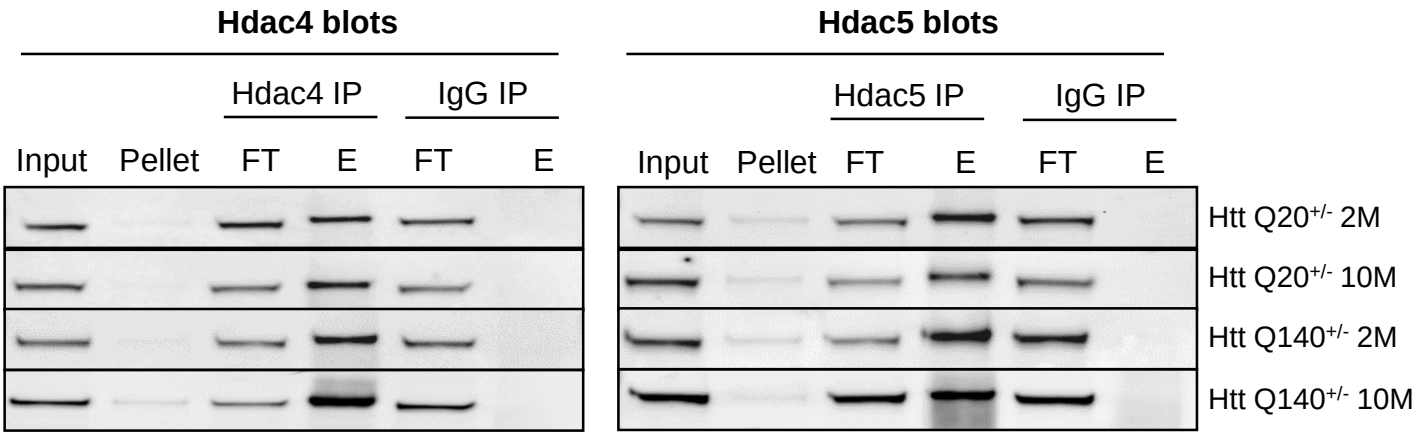

Figure S5. Striata IP efficiency blots. Western blots showing efficiency of Hdac4 and Hdac5 IP from HD mouse striata.

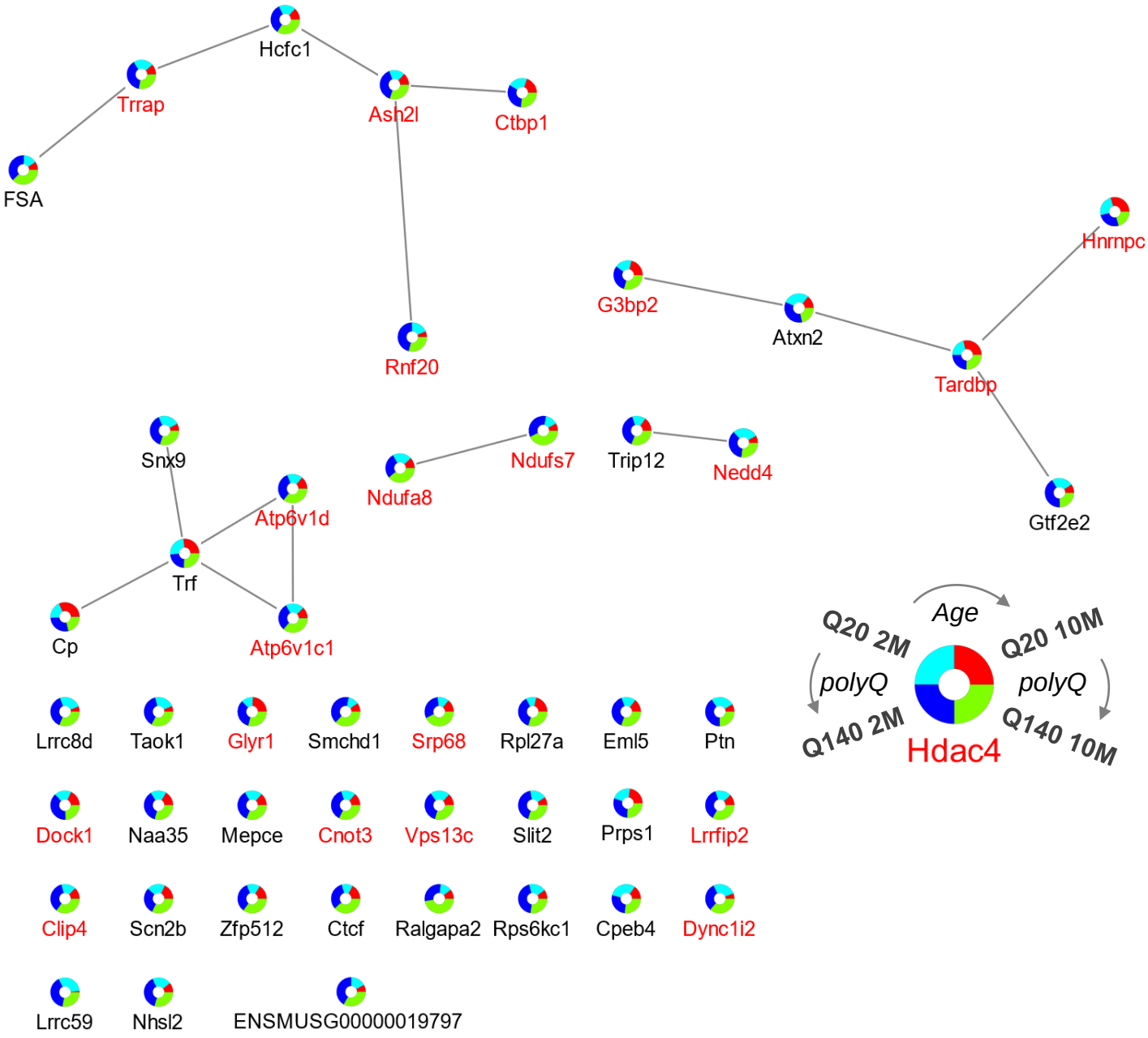

Figure S6. Additional specificity-filtered Hdac4 interactions in dissected striata. Hdac4 interactions in Q20 and Q140 mice at 2 and 10 months of age with SAINT specificity scores between 0.95 and 0.97. Each interacting protein is shown as a ring plot with the relative median MS1 abundance levels in each isolation condition depicted as indicated on the Hdac4 ring at the center of the network. Gene names shown in red are Hdac4 specific interactions that are also reported Htt interactions. Edges represent known protein-protein interactions and other associations present in the STRING database.

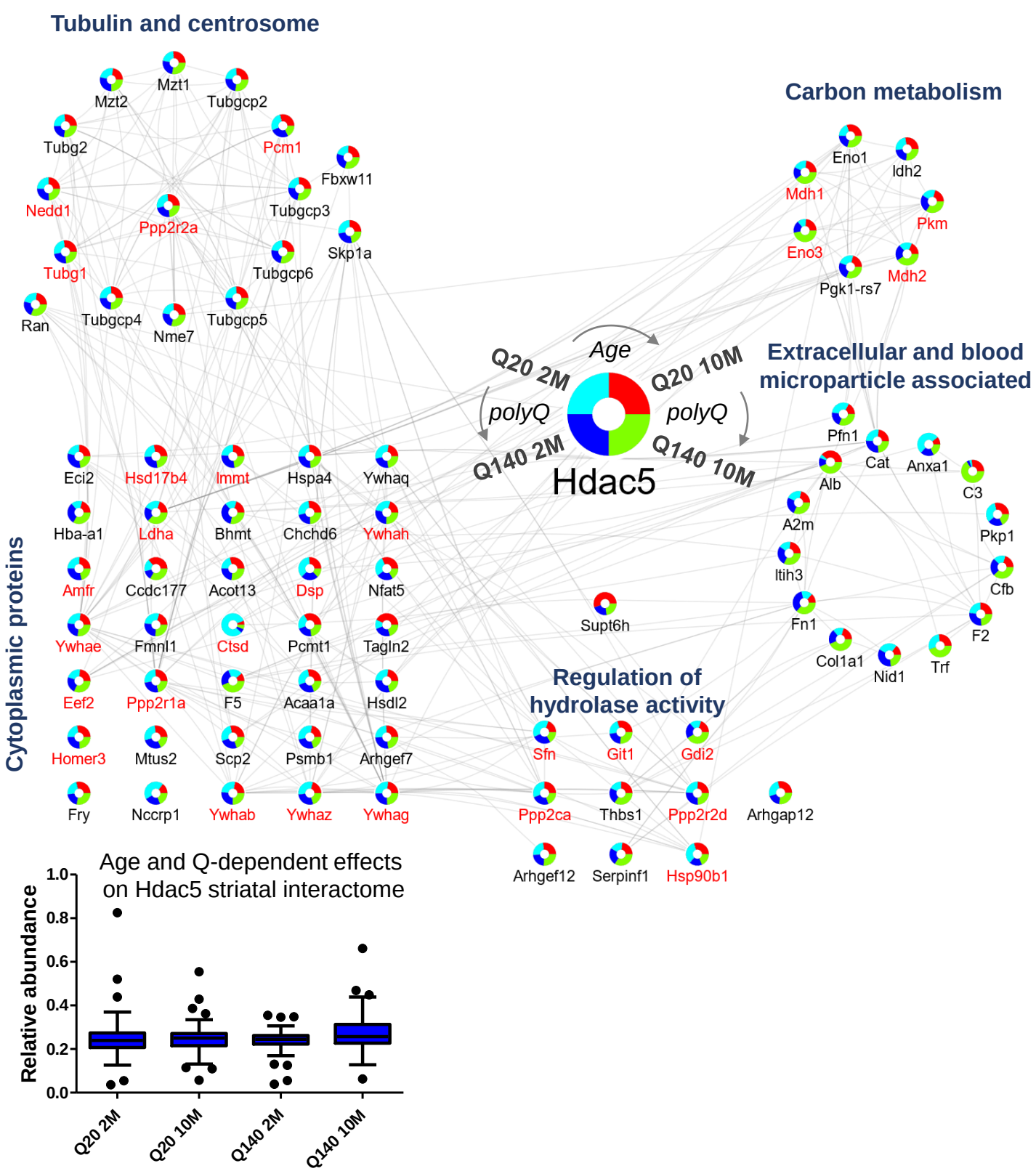

Figure S7. Hdac5 specificity filtered network in dissected striata. Comparison of endogenous Hdac5 interactions in Q20 and Q140 mice at 2 and 10 months of age. Each interacting protein is shown as a ring plot with the relative median MS1 abundance levels in each isolation condition depicted as indicated on the Hdac5 ring at the center of the network. Gene names shown in red are Hdac5 specific interactions that are also reported Htt interactions. Edges represent known protein-protein interactions and other associations present in the STRING database. Protein interactions have been functionally grouped and labelled in blue text. Inset boxplot shows overall Hdac5 interaction distribution in whole brain IPs.

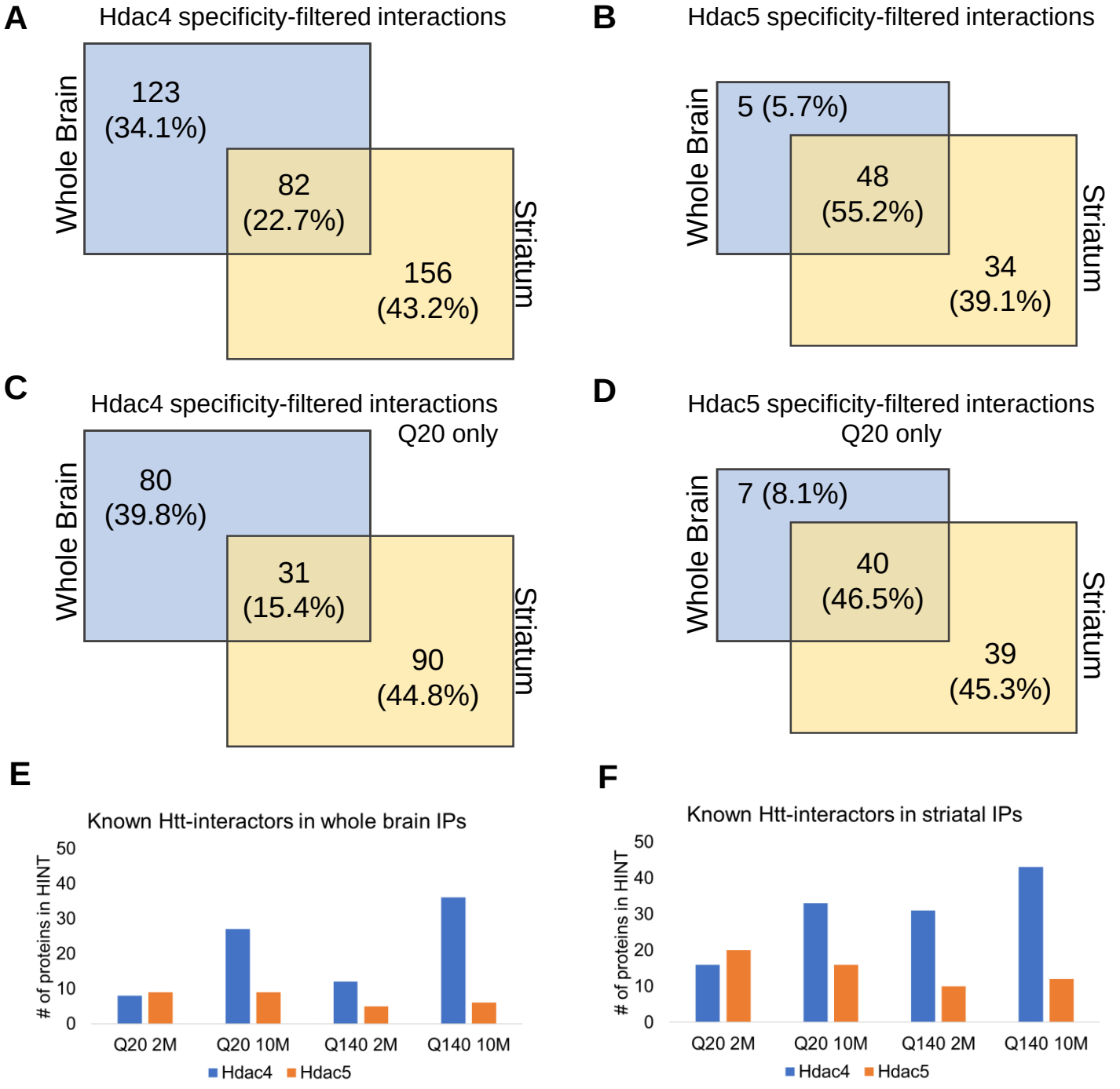

Figure S8. Comparison of whole brain and striata IPs. (A) Overlap of specificity-filtered Hdac4 interactions in whole brain and striata. (B) Overlap of specificity-filtered Hdac5 interactions in whole brain and striata. (C) Overlap of Q20 unique specificity-filtered Hdac4 interactions in whole brain and striata. (B) Overlap of Q20 unique specificity-filtered Hdac5 interactions in whole brain and striata. (E) Profile of known Htt-interacting proteins in Hdac IPs in whole brain. (F) Profile of known Htt-interacting proteins in Hdac IPs in striata.

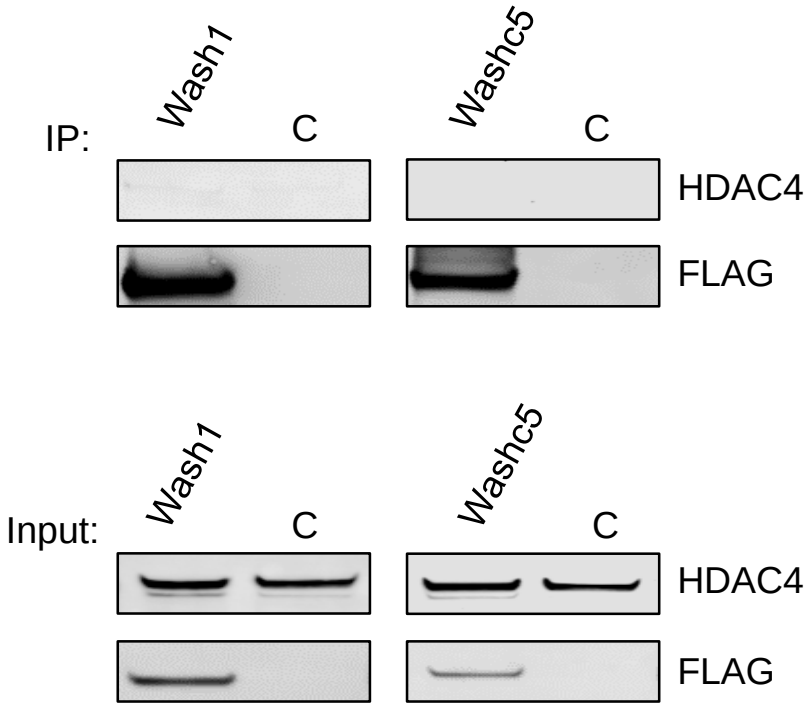

Figure S9. Reciprocal IPs of Wash1 and Washc5. Reciprocal isolations of FLAG-tagged Wash1 and Washc5 in HEK-293T cells did not co-purify HDAC4-GFP.

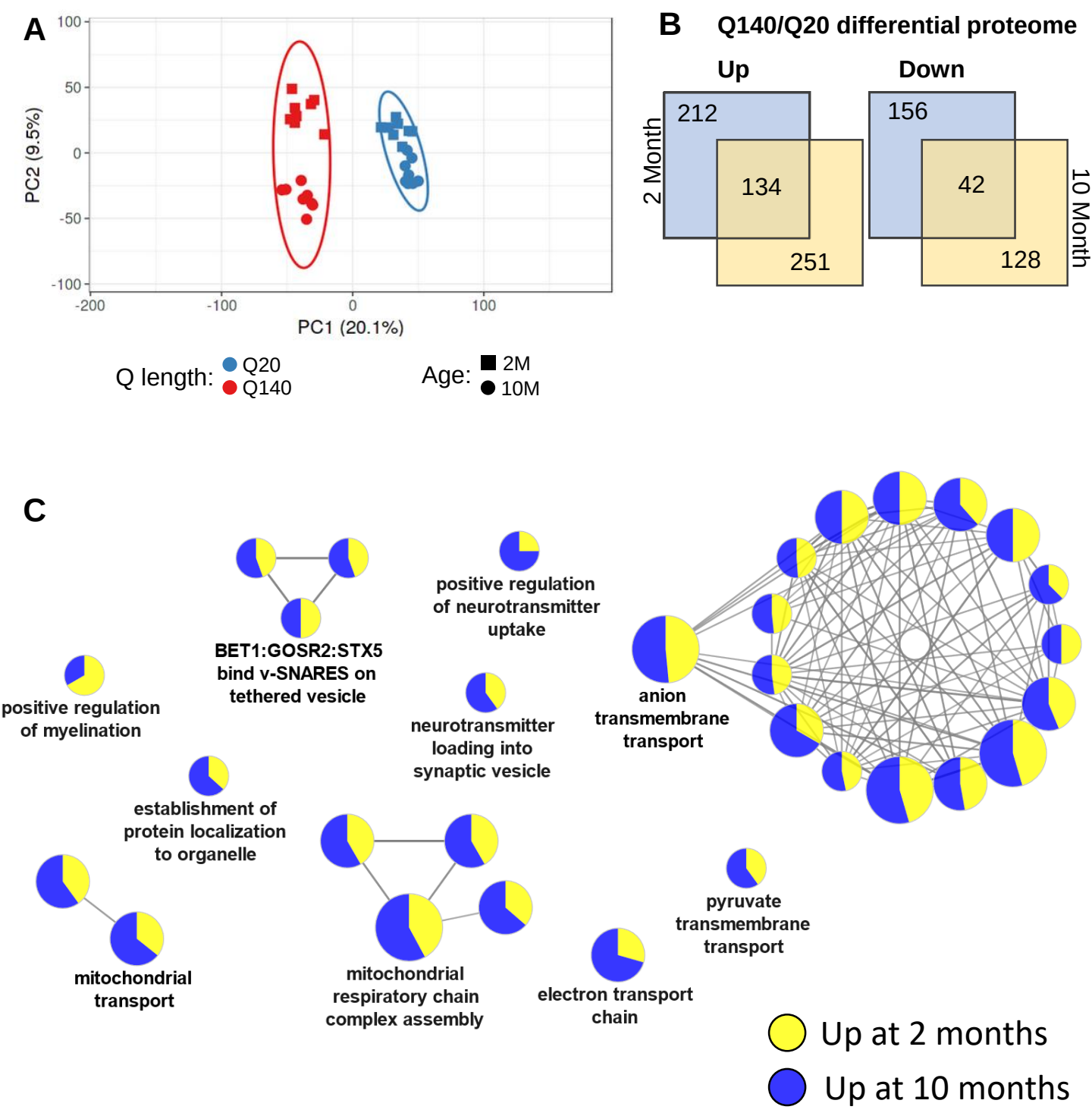

Figure S10. Examination of striatal proteome. (A) PCA reveals Q-dependent effects on striatal proteome. Age-dependent effects can also be seen in the Q140 mice. (B) Comparison of differential proteins at each age. (C) ClueGO analysis of up-regulated proteins reveals shared and enriched functional changes at each age.

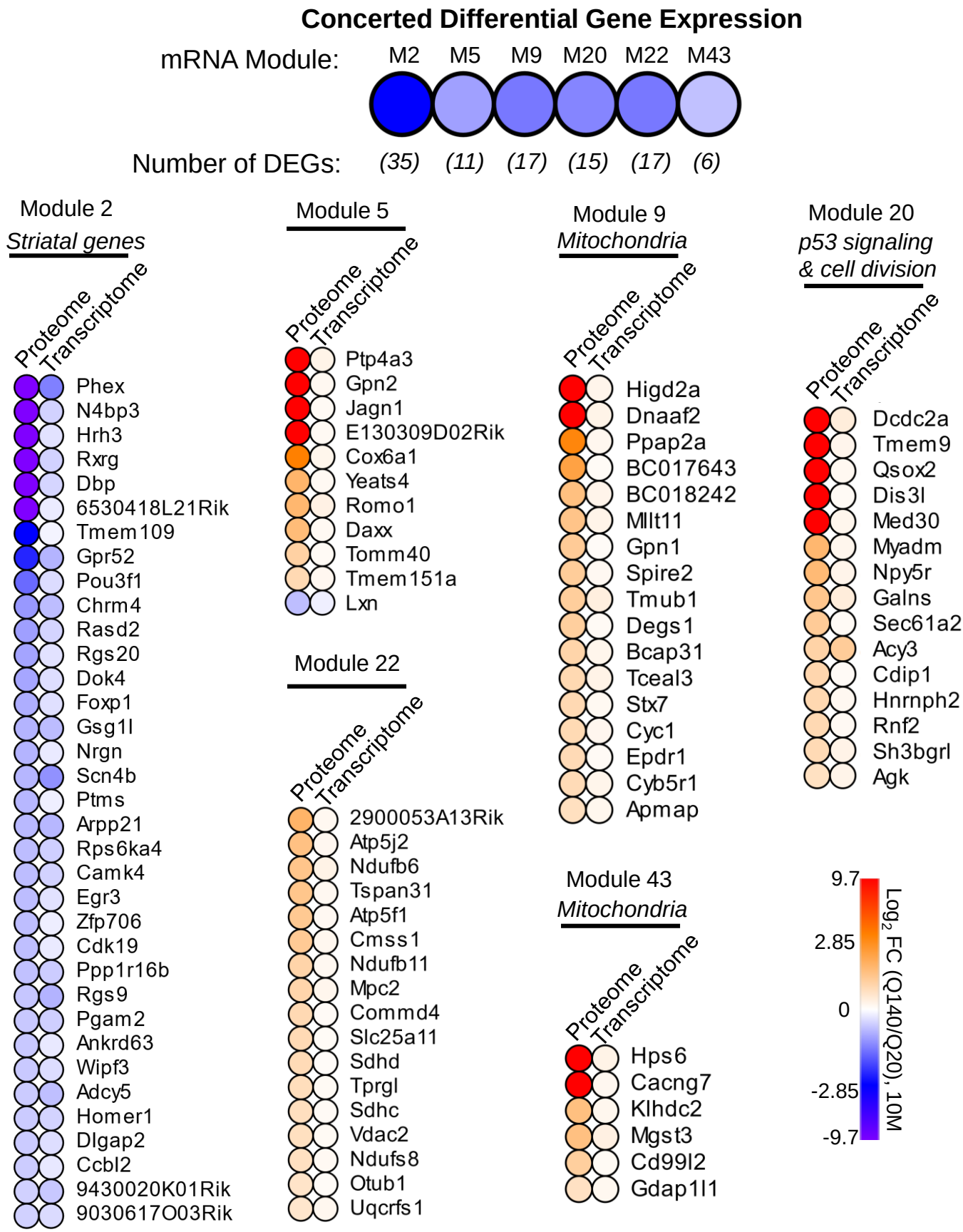

Figure S11. Comparison of concerted differentially expressed genes to previous data. Proteins and mRNA with concerted differential expression were compared to CAG-dependent mRNA modules defined in the Langfelder et. al. study. Previously defined modules that had more than 5 members in the 10 month proteome and transcriptome are shown. Modules with functions listed in italics were found to be significantly associated with CAG length in Langfelder et. al.

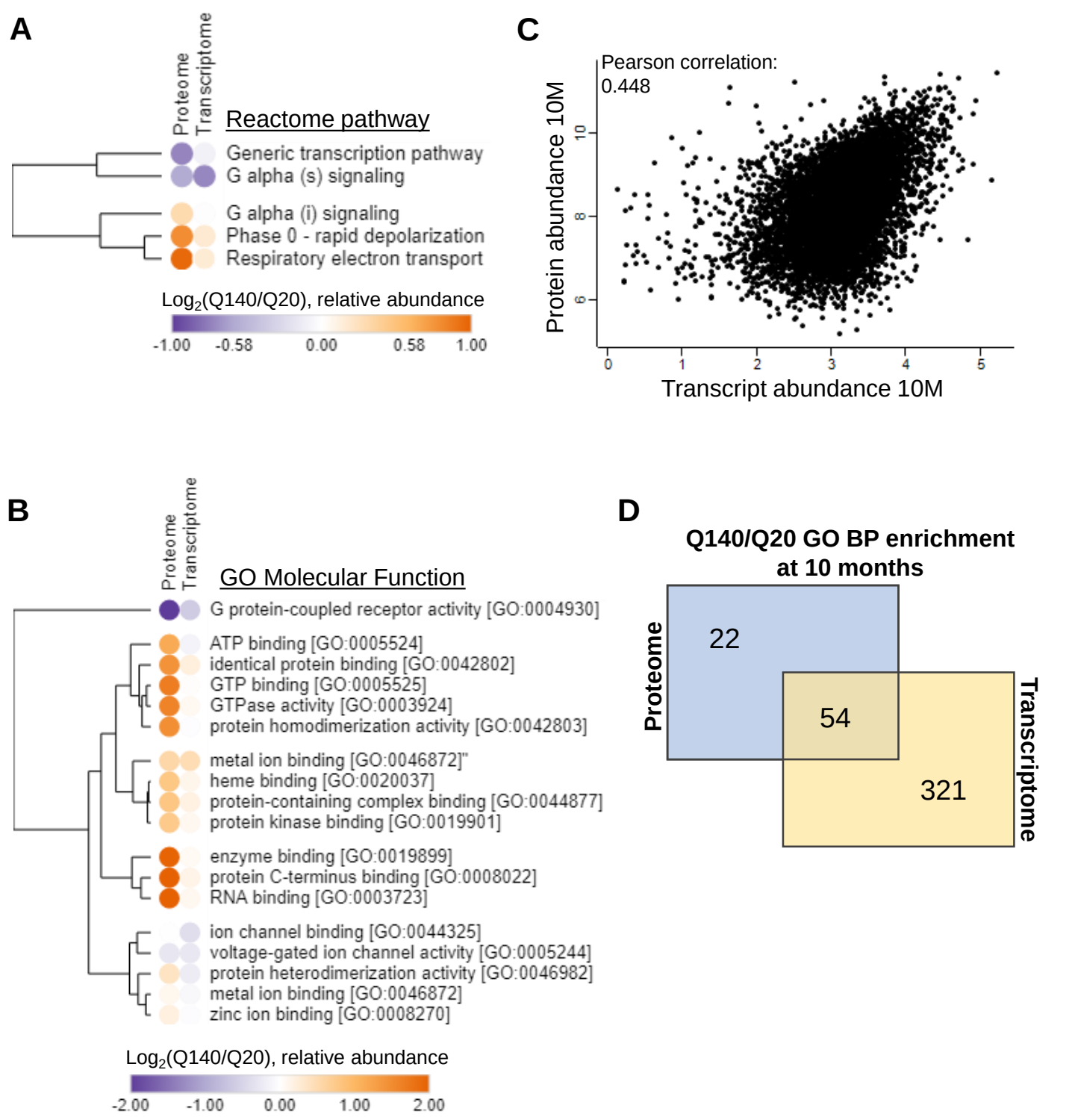

Figure S12. Multiomic analysis of HD striata. (A) Reactome analysis of genes with concerted protein and RNA changes. (B) GO molecular function analysis of genes with concerted protein and RNA changes. (C) Scatterplot of mRNA and protein abundance data shows Pearson correlation of 0.448. (D) Venn diagram of GO biological process enrichments in proteome and transcriptome up-regulated genes. v

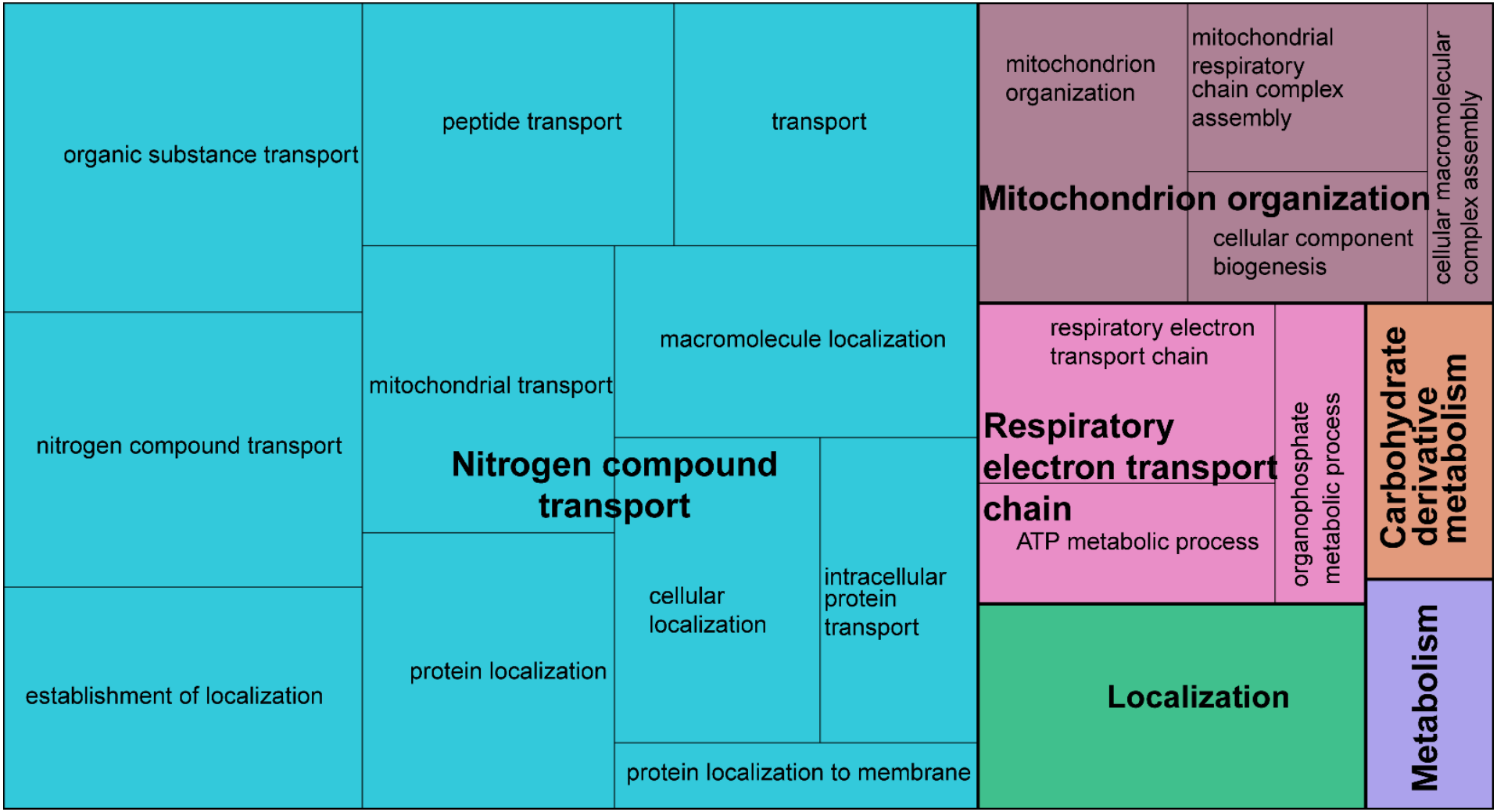

Figure S13. Proteome and transcriptome shared enriched GO terms. Treemap of shared GO term enrichments in both proteome and transcriptome for up-regulated proteins and RNA. Functionally related categories are grouped by color and boxes are sized by adjusted p-value.

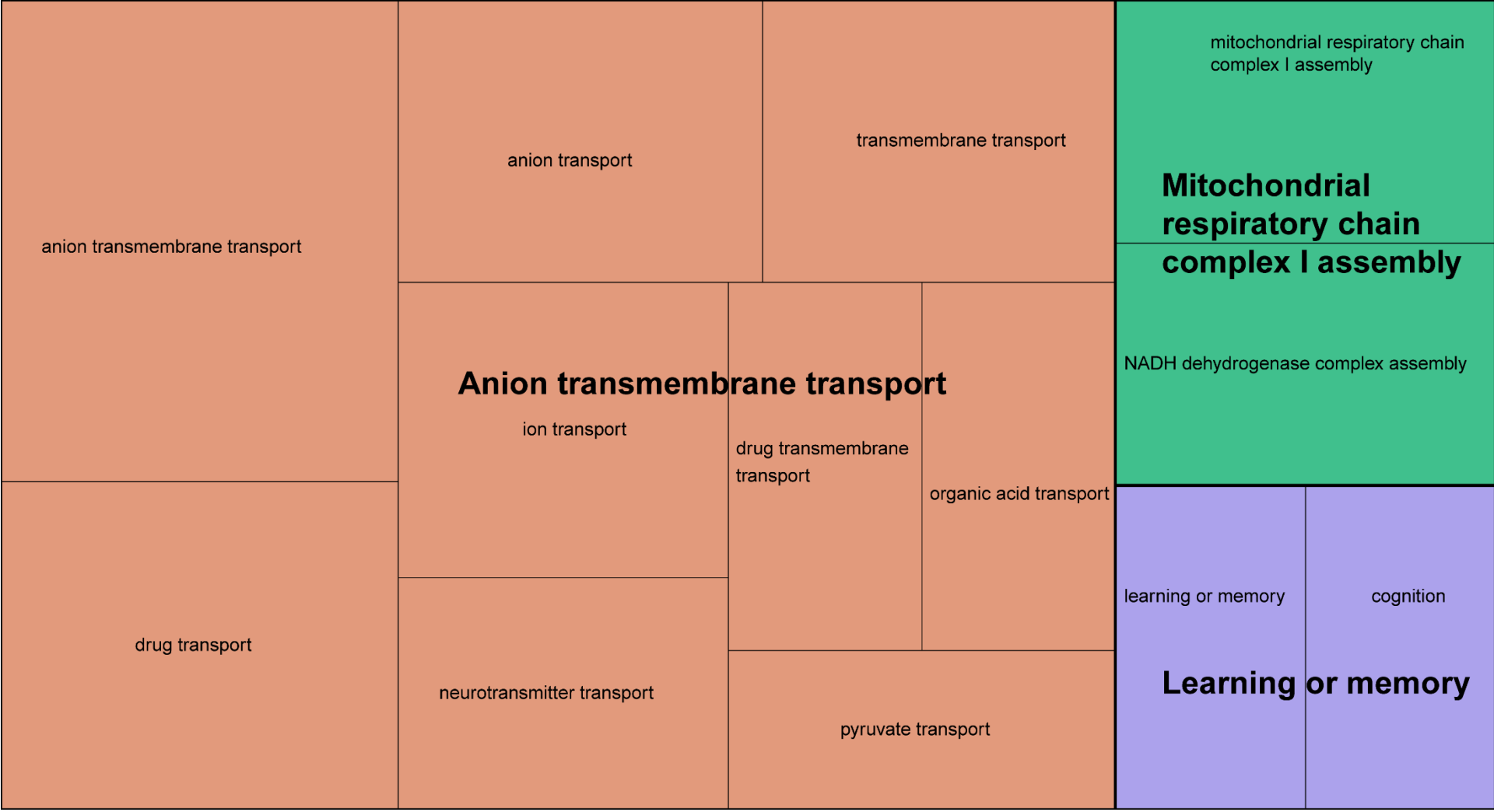

Figure S14. Proteome unique enriched GO terms. Treemap of proteome unique GO terms. Functionally related categories are grouped by color and boxes are sized by adjusted p-value.

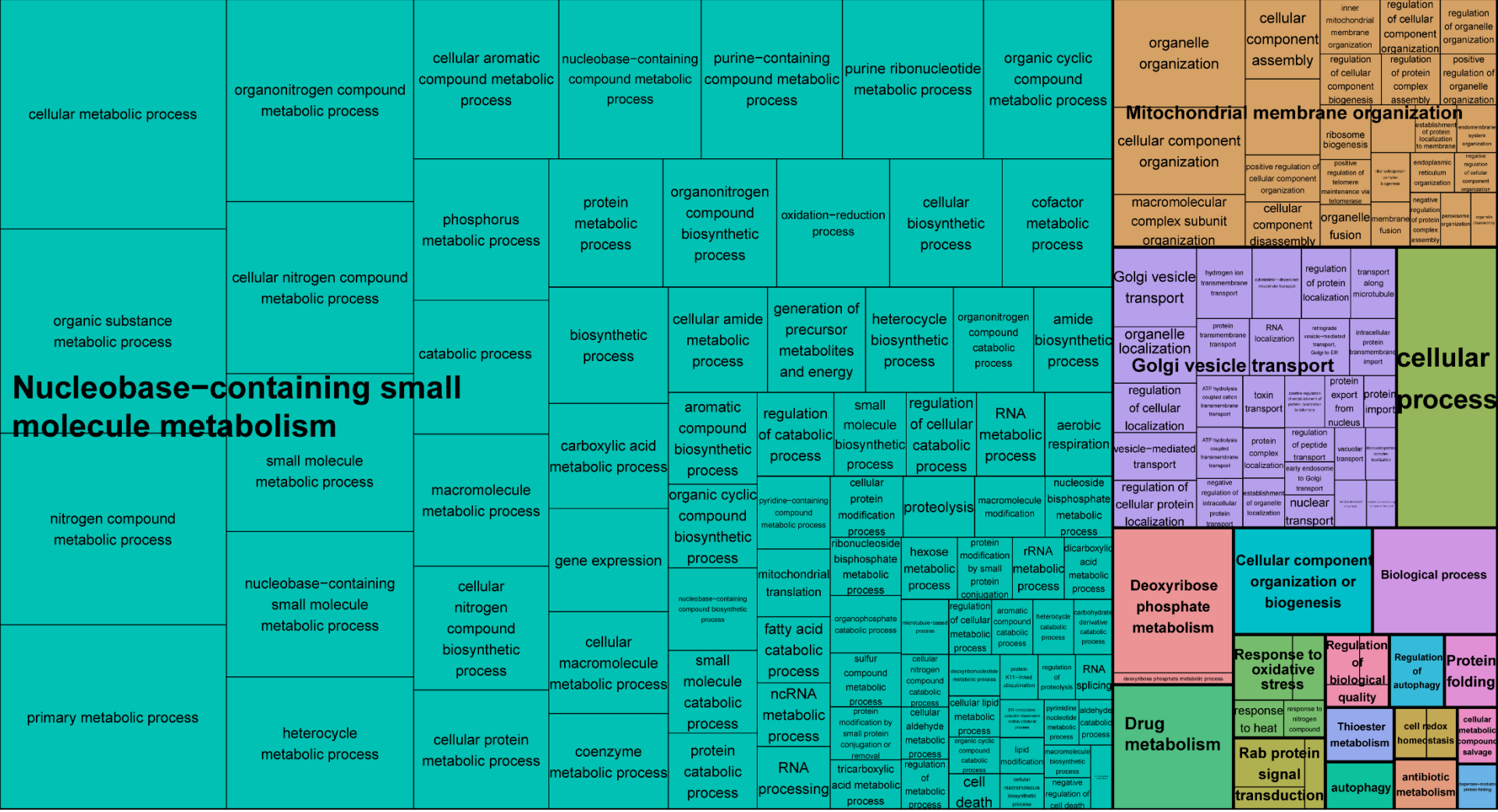

Figure S15. Transcriptome unique enriched GO terms. Treemap of transcriptome unique GO terms. Functionally related categories are grouped by color and boxes are sized by adjusted p-value.

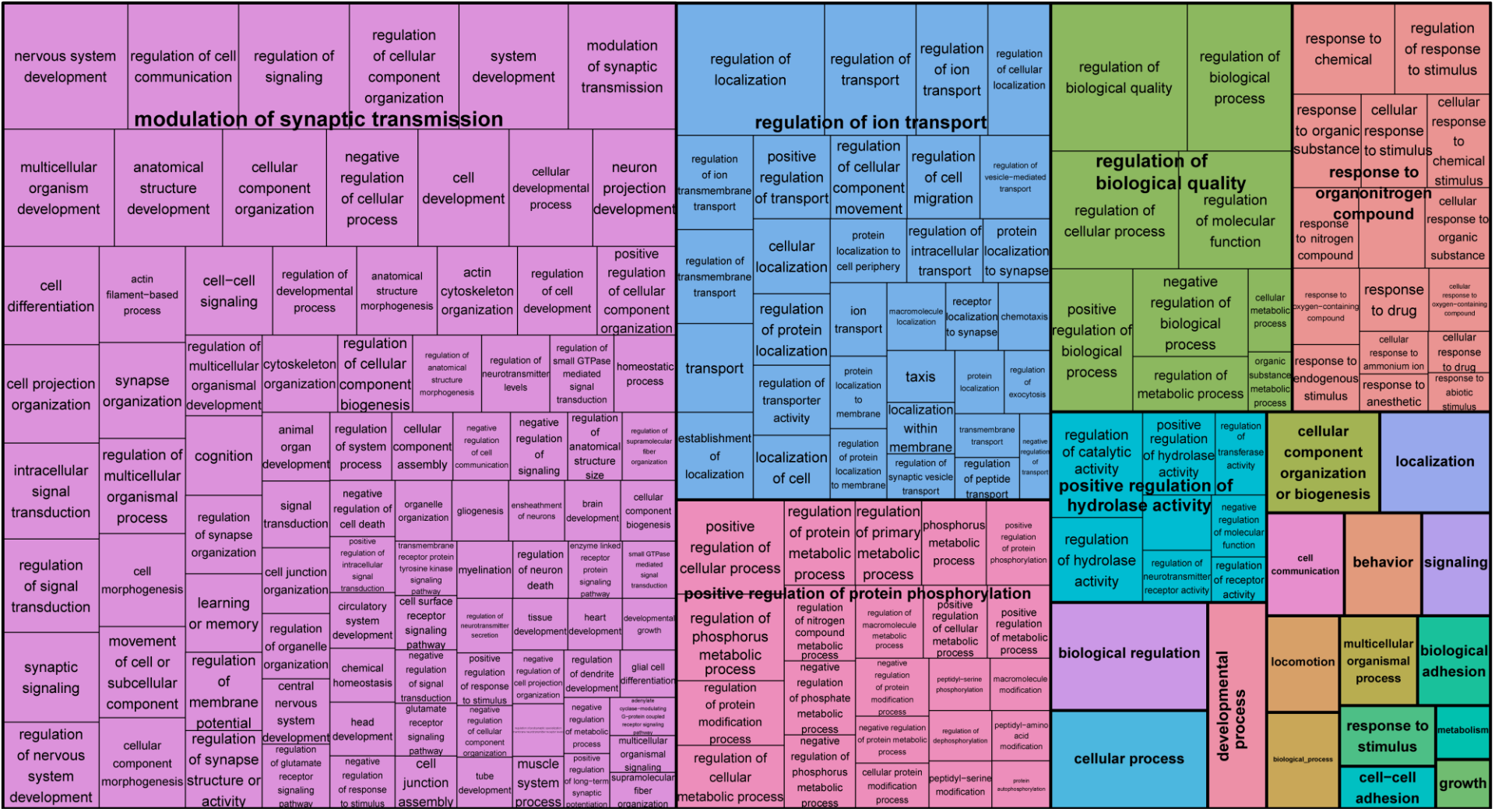

Figure S16. Downregulated transcriptome unique enriched GO terms. Treemap of transcriptome unique GO terms for genes that were significantly decreased in expression in Q140 10 month mice. Functionally related categories are grouped by color and boxes are sized by adjusted p-value.